sciendo

DOI 10.2478/ama-2023-0061

acta mechanica et automatica, vol.17 no.4 (2023)

EFFECT OF LUFFA SPONGE FIBRE MATS EMBEDDED IN THE PLASTER MATRIX

Khaled KHARRATI*,, Madiha SALHI*, Abdelmoumen HIDOURI***, Ridha ABDELJABAR***

*Research Lab TEMI, Faculty of Science, University of Gafsa, cité Sidi Ahmed Zarroug, Gafsa 2112 Tunisia
**National Engineering School of Gabes, University of Gabes, V432+8QR Zrig Eddakhlania 6029, Tunisia
***Institut Superieur of Technological Studies of Gafsa, University of Gafsa, Gafsa 2112, Tunisia

khaledkharrati27@gmail.com, salhimadiha2@gmail.com, abdelmomnhidouri@gmail.com, ridha.abdeljabar@enit.rnu.tn

received 16 March 2023, revised 18 May 2023, accepted 30 May 2023

Abstract: The present experimental research work aims to elaborate a new composite material (CM) composed of plasters reinforced with mats of long unidirectional luffa sponge fibres, treated chemically by 1% NaOH solution during 90 min at a temperature of 50°C, in orderto improve its thermomechanical and physical properties. The influence of fibre mat and fibre napping numbers of luffa sponge on density, porosity, flexural strength, thermal conductivity, thermal diffusivity, thermal effusivity and specific heat capacity properties was investigatedto lower building energy consumption. As far as our case is concerned, we processed a composite using single, double and triple-layer luffa sponge fibre mats. In our study, we are basically confined our experiments to three-layer mats. The experimental results revealed that the networking structure of fibres increases the flexural strength and decreases the thermal conductivity for a two-layer fibre wire mesh imbedded in the plaster matrix as compared with the neat plaster. However, there is a decrease in strength for a triple-layer composite, which referred to poor wetting of the fiber with the matrix material.

Key words: Luffa sponge fibre, reinforced plaster, mechanical characteristics, thermo-physical properties

1. INTRODUCTION

Gypsum materials were used for various applications hundreds of years ago and are still used to date. They are very cheap and suitable for multiple uses. However, nowadays, most of the surfaces inside building are either composed of synthetic or natural fibres or lined with gypsum products selected by architects for their high performance and outstanding qualities [1].

Gypsum (calcium sulphate dehydrate, $CaSO_4$, $2H_2O$) is frequently used as a finishing material in the construction and building industry owing to its feasibility, simplicity of application, fire resistance and environmental friendliness [2]. A gypsum network is formed when these crystals are implicated. Despite its numerous advantages, gypsum as a building material displays several disadvantages as well, including brittleness, weight and low water resistance [3, 4]. A composite material (CM) is a compound that is made up of two or more unique materials with diverse qualities on a macro scale to generate a new material with attributes that are completely different from those of the individual elements. A matrix is the basic phase of a CM with a continuous nature. In other words, the matrix corresponds to a substance that works as a binder, holding the fibres in place and transferring the external load to reinforcement. These matrices are considered as softer and more malleable. Notably, the main weakness of gypsum resides in its brittleness and poor mechanical properties, mainly under tension. Therefore, it is interesting to investigate different additives that can improve the mechanical properties of gypsum, focussing on the use of reinforcing fibres or additives in the gypsum matrix. Additionally, vegetable fibres also exhibit great tensile strength, toughness, extreme lightness and good thermal insulation properties with regard to their composition and structure [5]. These properties seem to favour construction material reinforcement. Most research works undertaken on vegetable fibres have been particularly oriented towards the improvement of mechanical properties of building materials.

Acda [6] performed a study on the mechanical resistance of CMs based on cement and natural additives. The inclusion of vegetable fibres in the concrete matrix can improve its mechanical strength [7]. Synthetic or natural fibres can be used as reinforcements. Several natural fibre-reinforced polymer composites (NFPCs) were introduced into the competitive market to meet the demand for growing environmental security. Basically, NFPCs outperform synthetic fibre-based composites in several ways. Since natural fibre composites have superior characteristics, these have grown in popularity and appeal [8].In 2021, Djoudi et al. [9] examined the physico-mechanical properties of CMs based on date palm tree fibres. Amelioration within the mechanical properties was reported corresponding to the fiber mass proportion up to 10%. In 2014, Djoudi et al. [10] investigated date palm fibers as a reinforcement in plasters. In consistency with the test findings obtained by these researchers, the consolidation of various concentrations of date palm fibres within the plaster increments the modulus of flexibility and water absorption. These outstanding properties indicating the low density of these fibres prompted many researchers to use these fibres for the development of bioderived composites [11–14].

Alcaraz et al. [15] explored the mechanical behaviour of materials composed of plaster and jute fabric, as well as the grip of jute fabric with plasters. The impact of jute fabric on the flexural, compressive and flexibility of the composite wasequally studied. They emphasised that the jute fabric reinforcement improves the

DOI 10.2478/ama-2023-0061

mechanical properties of the composite. They focussed on the improvement the mechanical properties of gypsum through the use of polymeric or metallic fibres. Eve et al. [16] mixed different concentrations of polyamide fibres with plasters. They asserted that all mechanical characteristics of the composite decrease with increasing fibre concentrations, except for fracture toughness. Gencel et al. [17] created a gypsum composite containing diatomite and polypropylene fibres. It is inferred that the addition of diatomite porosity contributes to reducing thermal conductivity and the addition of polypropylene fibres enhances mechanical properties. Loculano et al. [18] used treated hemp fibres as a reinforcement in gypsum boards. Results revealed increased toughness and reduced damage in low-impact tests. Basaran et al. [19, 20] investigated the behaviour of masonry walls with gypsum fortified in different ratios of polypropylene and steel fibres, which reinforced significantly the rigidity of walls. Khali et al. [21] reported gypsum plaster composites synthesised into plasters with different waste materials such as furnace slag, calcium carbonate and commercial alcohol polymer.The results demonstrated an increase in the compressive strength for lower concentrations of waste. The impact of chicken feather waste on thermal features of mortar composites was investigated by Ouakarrouch et al. [22]. They unveiled that chicken feathers enhance the thermal features of reinforced mortar. Sakthieswaran and Sophia [23] examined the mechanical characteristics of the *P. Juliflora* fibre reinforced gypsum composites and indicated that the flexural strength of the composites increases with the incorporation of 2% weight of *P. Juliflora* fibre, referring to the ability of the fibre to fill voids of the composites. Maaloufa et al. [24] opted forthe best percentage of cork and fibre in a gypsum matrix to optimise thermal insulation and mechanical properties. The thermal conductivity considerably improved. The alpha fibre enhanced the resistance to bending, but the cork makes the composite more vulnerable. Miraoui et al. [25] explored the effect of alpha fibres on the mechanical properties of mortar. They argued that alpha fibres improve the flexural strength of reinforced mortar. In 2019, Salim et al. [26] specified the mechanical characteristics of plaster-based composites with plastic fibres and glass powder. Furthermore, the fibre additions at various rates results in improvement in terms of mechanical properties. The thermal and mechanical performance of a gypsum composite reinforced with rice husk and oil palm trunk fibres was tackled by Selamat et al. [27]. According to the test results, the gypsum composite manufactured with 20% fibre loading has good thermal and mechanical stability. In this respect, Touil et al. [28] assessed the influence of alpha fibres on thermal-mechanical characteristics of the plaster. The results suggested that by increasing the fibre concentration, the thermal features can be significantly enhanced. The mechanical assays, on the other side, indicated that adding fibres to the plaster permits a reduction in its resistance to bending, but an enhancement in the failure mechanismleads to a nonlinear and ductile behaviour.

In this research paper, our central focus is on the physico-thermo-mechanical properties of bio-CMs made up of plasters and luffa sponge fibres. Fibres wire meshes are formed into mats of various layers that are embedded in a matrix of plasters such that they act together to resist forces. The major purpose of reinforcement is to provide additional strength for plasters where it is needed, as well as toexplore the physical and thermal properties of CMs.

2. MATEIALS AND METHODS

2.1. Materials

2.1.1. Plaster

The plaster used for the study was KNAUF maknessy plaster (staff plaster), which is noted for its simplicity of application and exceptional degree of finishing that can be put manually on all supports [En fait, ce matériau est connu par sa facilité d'application et aussi par son degré exceptionnel de finition, s'appliquant ainsi manuellement sur tous les supports]. The plaster is derived from gypsum through the heating process, as described in the following Eq. (1):

$$CaSO_4.2H_2O + Heat \longrightarrow CaSO_4.1/2H_2O \quad (1)$$

X-ray diffraction allowed us to better investigate the mineralogical composition of plasters. Fig. 1 illustrates the diffractogram that characterises the different mineralogical components of anhydrous plasters. It reveals that the plaster in our study is composed of some elements, which are indicated in Tab.1. The percentages of the elements making up the plaster are provided using TOPAS software, which is based on Rietveld analysis.

Tab. 1. Mineralogical composition of plaster

Mineralspecies	Formula	Content (%)
Bassanite	$CaSO_4.0, 5H_2O$	92.43
Calcium sulphate	$Ca(SO_4)$	4.14
Dolomite	$CaMg(CO_3)_2$	3.43
Crystallinity rate		78.6

2.1.2. Luffa sponge

Luffa is a climbing plant in the Cucurbitaceae family, and its dry fruit (luffa sponge) has a fibrous net-like vascular system (see Fig. 2).

Relying on previous studies [29, 30], the percentages of alkaline solution rates, such as, 0.5%, 1%, 2%, 3% and 5%,were selected to better enhance fibre characteristics. The alkaline treatment targeted the changes in chemical compositions of luffa sponge fibres [41]. The cellulose content in treated luffa sponge fibre increased while hemicellulose and lignin contents decreased as compared with untreated luffa sponge fibres. It corresponds to one of the treatment methods commonly applied to adjust the surfaces of natural fibres in order to enhance the interface compatibility among fibre and plaster matrixes. It induces a better contact and bonding mechanism between fibre and plaster matrixes.

The treatment was carried out through performing a series of chronological steps under laboratory conditions. These steps are described as follows.

First, the dry luffa sponge (see Fig. 2 (a)) was anatomised longitudinallyto transform it into a parallelepiped shape instead of a cylindrical one (see Fig. 2 (b)). Then, it was cut into rectangular webs of predefined dimensions (see Fig. 2 (c)). Subsequently, these luffa sponge webs were chemically treated under different conditions. Then, they were dried. In this way, the luffa sponge fibres could be easily extracted from the web. Finally, these fibres were cut according to the required dimensions (see Fig. 2 (d)).

DOI 10.2478/ama-2023-0061

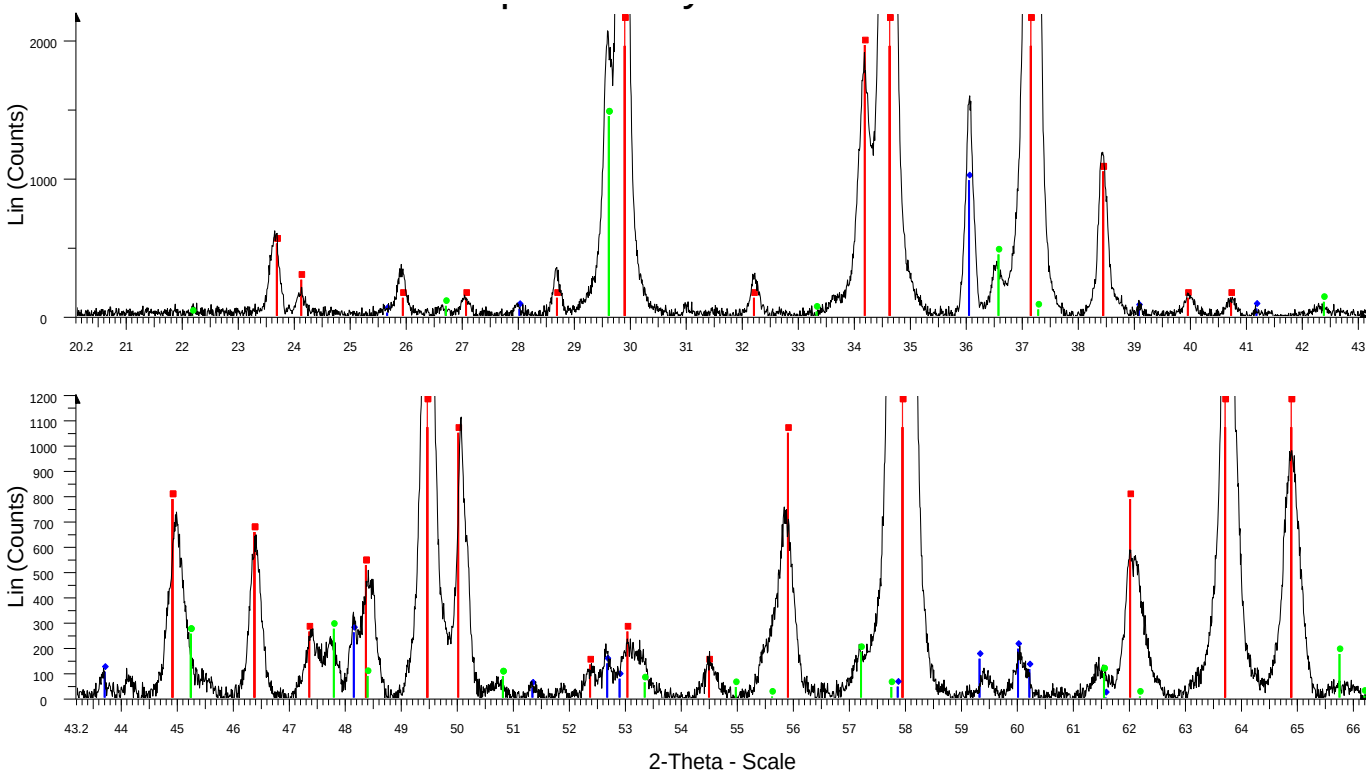

Fig. 1. X-ray diffraction analysis of anhydrous plaster (Meknassy)

Fig. 2. (a) Luffa sponge, (b) The portion of the luffa open as mat, (c) luffa mat and (d) luffa fibres

The fibers must, first of all, be washed with hot distilled water at a temperature T= 40°C so as to remove any natural hazards (dust, dirt, etc.). They were next dried in an electric oven. Subsequently, the specimens were soaked in different concentrations of NaOH solutions: 0.5%, 1%, 2%, 4% and 5%, at different temperatures (25°C, 50°C and 75°C) and different time intervals (1/2 h, 1h, 3/2h, 2h and 3h), as demonstrated in Fig. 3. After finishing the treatment operation with the NaOH solution, some contaminations related to this operation may appear on the luffa sponge fibre surfaces. These contaminations may equally have a negative impact on the quality of these fibres. To shun this risk, we resorted to wash the fibres well several times (3–4 times) using hot distilled water T= 40°C in order to remove all remaining NaOH residues to reach a neutral pH. Afterwards, the fibres were dried at a temperature of 50°C, for 7 h.

DOI 10.2478/ama-2023-0061

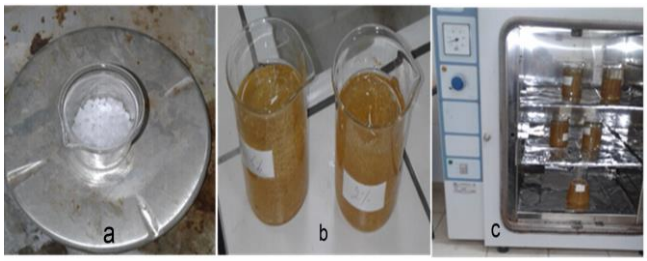

Fig. 3. Step of laboratory treatment: (a) NaOH solid, (b) NaOH solution and (c) fiber soaking in NaOH solution in oven

The tensile strength of treated fibres under various conditions, such as concentration of alkaline solution, time of soaking and temperature, was assessed. It has been found that the fibres drenched in an alkaline solution of 1% NaOH concentration for 90 min at 50°C temperature, which are regarded as an optimum condition, bring about an increase in the rate of tensile strength of around 61% as compared with the untreated fibre. Fig. 4 outlines the obtained results.

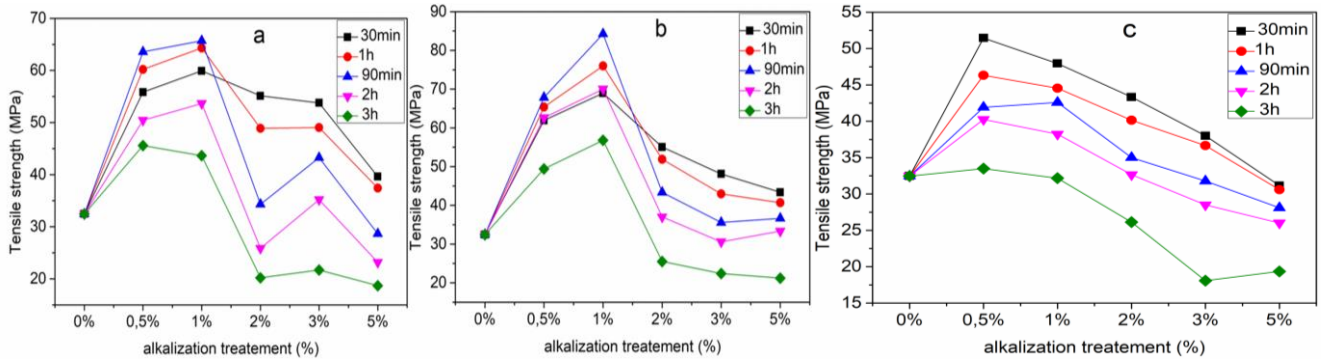

Fig. 4. The effect of NaOH on the tensile strength of luffa sponge's fibers treated with different concentrations and duration (a) for 25°C, (b) for 50°C and (c) for 75°C [31]

2.2. Experimental methods

2.2.1. Fibres preparation

Mathematical formulas should be type written in mathematical style, aligned to left and numbered irrespective of chapter numbering.

After cutting fibres manually from luffa sponge into rectangular mats, they are soaked in an alkaline solution of 1% NaOH concentration for 90 min at 50°C. After being dried, the outer core and a micro channel section of the sponge guard were opened without regard to the end portion so as to maintain the same thickness of the mat, as portrayed in Fig. 5 (a) (luffa sponge fibre mats were invested to manufacture the layered composite; see Fig. 6).

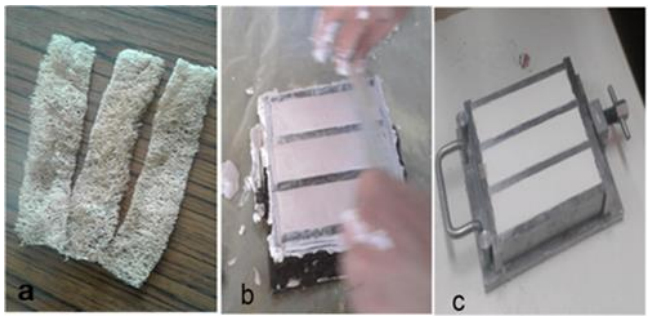

Fig. 5. (a) The luffa part in the form of a rectangular shape with dimensions (150mm- 30mm- 5mm) and mass (1.85g), (b) Hand scraping the surface of the filled mold and (c) three identical specimens preparation

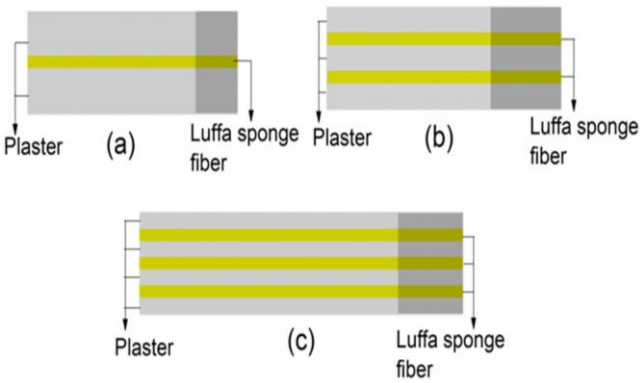

Fig. 6. Graphic views of the composites : (a) Single layer composite (SL), (b) Double layer composite (DL) and (c) Triple layer composite (TL)

2.2.2. Plaster matrix preparation

The preparation of a blend of mortar was carried out through blending plasters with water, utilising a water-to-plaster proportion (w/g) of 0.6 in the blending method. Afterwards, the specimens were put away and dried for 28 days at laboratory ambient temperature.

In our case, we did this through selecting a composite using single-layer (SL), double-layer (DL) and triple-layer (TL) luffa sponge fibre mats, as shown in Fig. 6. We cannot opt for more than three-mat layers, as the thickness does not match the total height of the specimens. Four different specimens for various layers (neat plaster, SL, DL and TL) produced in three examples were tested, as shown in Fig. 5 (c). In total, 12 specimens were tested

2.2.3. Flexural strength

Flexural tests were conducted with a three-point bending device.The specimens were manufactured with a dimension (40 mm × 40 mm × 160 mm, see Fig. 7) in accordance with the requirements of NF EN 196-1, which is the standard determined for mechanical tests (three-point bending, Fig. 8). The machine was computer controlled, with a constant speed loading of 2 mm/min until the material broke down.
The flexural strength is denoted by the following Eq. (2):

$$R_f = \frac{3 \times F_f \times L}{2 \times b \times h^2} \quad (2)$$

where: R_f is flexural strength (MPa), F_f is force applied (N), b is the width of specimen (mm), h is the thickness of the specimen (mm) and L is the length of the specimen (mm).

When the specimen gives up bending, this corresponds to a yield point.

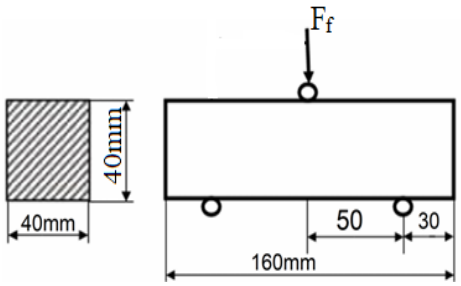

Fig. 7. Three points bending test machine

Fig. 8. Sketch of Device for the three-point bending strength test

2.2.4. Porosity calculation

The experimental method invested in this work to determine the porosity of specimens was identified in the following steps. First, we weighed each specimen in the dry state with an electronic balance. Second, each specimen was dipped in distilled water for 48 h. Third, each specimen was weighed in the wet state; then, the void volume of each specimen was specified by computing the difference between the wet mass and the dry solid mass. Finally, the void volume of each specimen was estimated through computing the difference between the wet mass and the solid mass and then dividing by the density of water. The porosity was obtained according to the following Eq. (3):

$$P = \frac{void\ volume}{Total\ volume} \times 100 \quad (3)$$

where: P expresses porosity (%).

2.2.5. Density

The density (ρ) of the materials was evaluated after they had dried. It stands for the mass unit volume of the material that makes up the aggregate, considering the voids that may exist within or between the grains. The density (ρ) is computed using the following Eq. (4):

$$\rho = \frac{M}{V} \quad (4)$$

where: M is the total mass of specimen (g) and V is the volume of the specimen (cm^3).

2.2.6. Thermal apparatus

The “blue box” LEI700 measurement cell was used to determine this procedure. The measurement instrument was made up of a well-insulated box called “A” that was kept cool by glycol water flowing from a cryostat. Two identical and independent measurement boxes, namely “B1” and “B2,” were insulated with polystyrene inside and invested to measure steady-state thermal conductivity and transient thermal diffusivity, respectively (see Fig. 9).

Fig. 9. Photo of EI700 measuring Apparatus

2.2.6.1. Thermal conductivity

Measuring thermal conductivity using the box method in the steady state rests on creating two atmospheres: hot and cold, on both sides of the material to be tested (a low temperature and highly insulated enclosure), and a box is equipped with a heating film controlled by a rheostat in order to maintain a temperature close to ambient temperature. The surface temperatures of the specimen of lathhot and cold face as well as the ambient temperature were controlled and measured, as displayed in Fig. 10. When the temperatures stabilise with variation of the order of 0.1° in 1 h, we suppose that the steady state is achieved. This lies basically between 4 h and 7 h after mounting the specimen.

The thermal conductivity is provided by the following Eq. (5):

$$\lambda = \frac{e}{S(T_C - T_F)} \left[\frac{U^2}{R} - C(T_B - T_A) \right] \quad (5)$$

DOI 10.2478/ama-2023-0061

where: e is the thickness of the sample (m), S is the area of the sample (m^2), A is the value of the heating resistor (Ω), C is the heat loss coefficient (W/K), U is the voltage across the resistor (V), T_C and T_F are the temperatures of the hot side and the cold sides (°C), respectively, and T_B and T_A are temperatures inside the box and ambient temperature (°C), respectively.

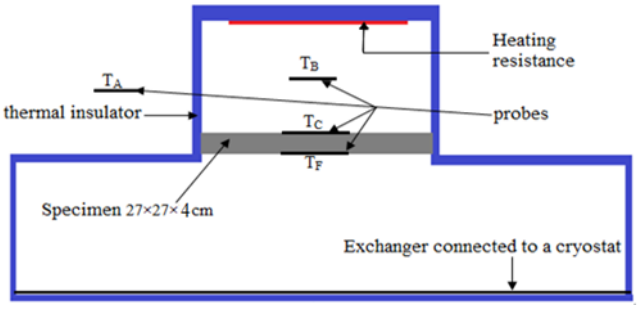

Fig. 10. Descriptive diagram of the device for measuring thermal conductivity

2.2.6.2. Thermal diffusivity

As for the measurement of thermal diffusivity in a transient state, a measurement cell is composed of two identical boxes, perfectly symmetrical (see Fig.11) and strongly insulated from the external environment by polystyrene. To send a heat flux, a constant high-power halogen lamp (1,000 W) was used for a controlled duration on the upper face of the specimen.The thermal diffusivity was deduced departing from the experimental thermogram (Fig. 12), using the DEGIOVANNI model.

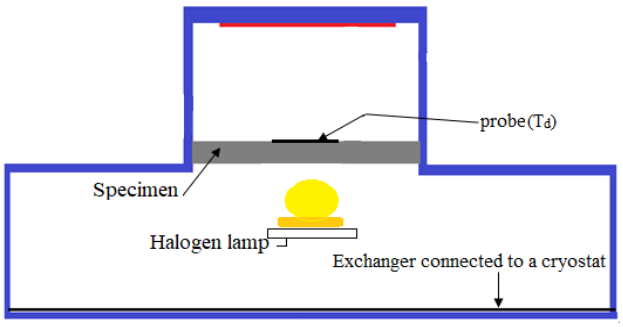

Fig. 11. Descriptive diagram of the device for Thermal diffusivity measurement

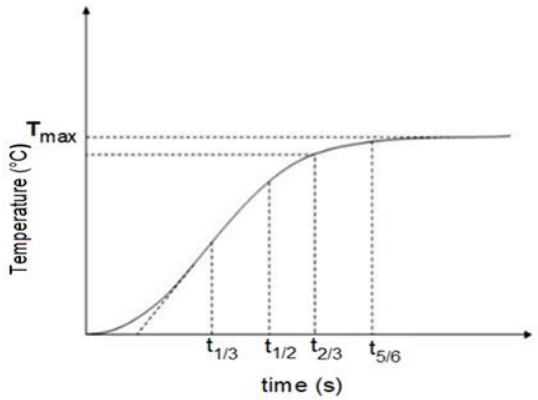

Fig. 12. Typical thermogram for the determination of thermal diffusivity [39]

DEGIOVANNI model

Actually, in order to specify the thermal diffusivity, we applied the DEGIOVANNI model [39]. Eq. (9) makes it possible to estimate the thermal diffusivity by knowing the times for which several pairs of points were considered, at characteristic times: $t_{1/3}$, $t_{1/2}$, $t_{2/3}$ and $t_{5/6}$. In addition, we need to take into account heat losses during diffusivity measurement [32].

$$\begin{cases} \alpha_1 = \dfrac{e^2}{t^2_{\left(\frac{5}{6}\right)}}\left(\left(1{,}15 \times t_{\frac{5}{6}}\right) - \left(1{,}25 \times t_{\frac{2}{3}}\right)\right) & (6) \\ \alpha_2 = \dfrac{e^2}{t^2_{\left(\frac{5}{6}\right)}}\left(\left(0{,}761 \times t_{\frac{5}{6}}\right) - \left(0{,}926 \times t_{\frac{1}{2}}\right)\right) & (7) \\ \alpha_3 = \dfrac{e^2}{t^2_{\left(\frac{5}{6}\right)}}\left(\left(0{,}761 \times t_{\frac{5}{6}}\right) - \left(0{,}862 \times t_{\frac{1}{3}}\right)\right) & (8) \\ \alpha = \left(\dfrac{\alpha_1 + \alpha_2 + \alpha_3}{3}\right) & (9) \end{cases}$$

2.2.6.3. Thermal effusivity

One of the prominent ideas regarding how thermal insulation materials operate is thermal effusivity. It corresponds to the material's capacity to both absorb and release heat from its surface. Materials with high thermal effusivity cannot retain heat for very long since they lose it rapidly from their surface when the surrounding temperature decreases.

Thermal effusivity [37] of the CMs was calculated according to the Eq. (10) by determining the experimental values of thermal conductivity and thermal diffusivity.

$$E = \frac{\lambda}{\sqrt{\alpha}} \quad (10)$$

where: E is thermal effusivity (J · K^{-1} · m^{-2} · s$^{-1/2}$), λ is thermal conductivity (W · m^{-1} · K^{-1}) and α is thermal diffusivity (m^2 · s^{-1}).

2.2.6.4. The specific heat capacity

An intrinsic factor that characterises the thermal inertia of materials is the specific heat capacity. It is obvious to determine the specific heat capacity of CM whenever its density, thermal conductivity and diffusivity are computed. The relationship is provided as follows:

$$C_p = \frac{\lambda}{\rho \cdot \alpha} \quad (11)$$

where: C_p is specific heat capacity (J · kg^{-1} · K^{-1}) and ρ is density (kg · m^{-3}).

3. RESULTS AND DISCUSSION

The experimental findings for each specimen are outlined in Tab. 2.

Tab. 2. Test results

Specimen	Porosity (%)	Flexural Strength (MPa)	Density ($kg \cdot m^{-3}$)	Thermal diffusivity ($m^2 \cdot s^{-1}$)	Thermal Conductivity ($W \cdot m^{-1} \cdot K^{-1}$)	Thermal effusivity ($J \cdot K^{-1} \cdot m^{-2} \cdot s^{-1/2}$)	Specific heat capacity ($J \cdot kg^{-1} \cdot K^{-1}$)
Plaster	38±0.7	1.3±0.02	1168±8	2.8±0.011 10^{-7}	0.27±0.002	510.25±3	825.58±2
Plaster+ SL	43±0.9	1.5±0.03	1103±9	2.7±0.012 10^{-7}	0.252±0.003	484.97±4	846.18±2.7
Plaster+ DL	47±0.8	1.6±0.02	1048±8	2.61±0.01 10^{-7}	0.236±0.002	461.95±3.5	862.8±2.3
Plaster+ TL	54±1	1.4±0.04	983±9	2.49±0.013 10^{-7}	0.215±0.003	430.86±4.3	878.39±2.8

4. MECHANICAL PROPERTIES

4.1. Behaviours of plaster are reinforced with mats of long unidirectional luffa sponge fibres

A load deflection curve for plasters with and without reinforcement is depicted in Fig. 13. The behaviour of reinforced plaster is characterised by DL luffa sponge fibre mats, as shown in Fig. 13 (plaster + DL):

1. The first region presents a non-linear behaviour. It corresponds to the behaviour of a pure plaster (matrix).
2. The second zone is an intermediate zone from which there may be a slight load drop corresponding to the first macroscopic damage to the composite. Then, the load is taken up by luffa fibre mats up to the maximum strength.
3. The third region corresponds to the manifestation of nonlinear behaviour from the maximum force applied to the test sample. One notes a slight reduction in load associated with tearing and damage to the reinforced plaster.

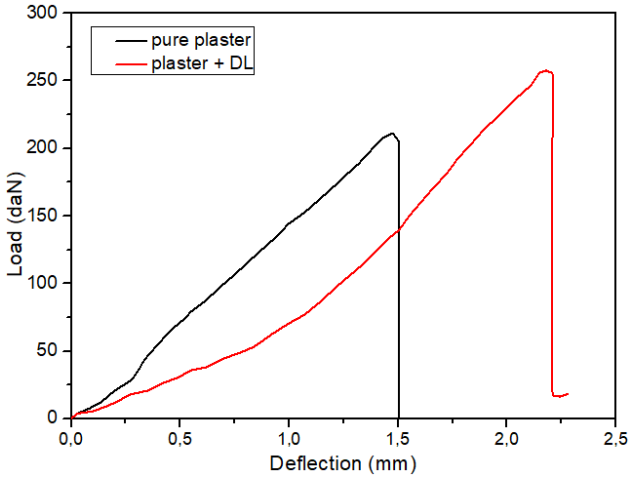

Fig. 13. Load deflection curve: Plaster with reinforced mats of long unidirectional Luffa sponge fibers, pure plaster

The specimen behaviour reinforced with luffa fibre mats displays an improvement in deflection at failure, see Fig. 13 (plaster + DL) and (pure plaster).

Fig. 14 illustrates the failure stages of unidirectional long luffa fibre mat-reinforced plasters after the three-point bending tests. One notices that the reinforced plaster is cracked first; then, the load is carried by the fibres up to F_{max}. Next, failure occurs as the luffa fibres slip, see Fig. 14.

Fig. 14. Failure stages of plaster reinforced with mats of long unidirectional Luffa sponge fibers

4.2. Flexure tests

The specimens were subjected to a three-point flexural test. The flexural tests in Fig.15 revealed that the plaster with fibre mats resisted to flexural strength more than specimens of pure plaster. According to the test results, a change in the flexure behaviour was observed during each test. A maximum resistance was detected for a specimen with DL. The maximum flexural strength and deflection were 1.6 MPa and 2.2 mm, respectively, as shown in Fig.13. It was inferred that with the addition of luffa fibre mats, the mechanical features of CM improved. It was observed that various layers of fibre mat reinforcement had different failure and deflection impacts on the CM. There was no significant change in terms of bending, but stiffness, strength and ductility enhanced with the addition of fibres mats. Similar observations were reported by Babu et al. [33] and Djoudi et al. [34], while they had been working on reinforced fibres.

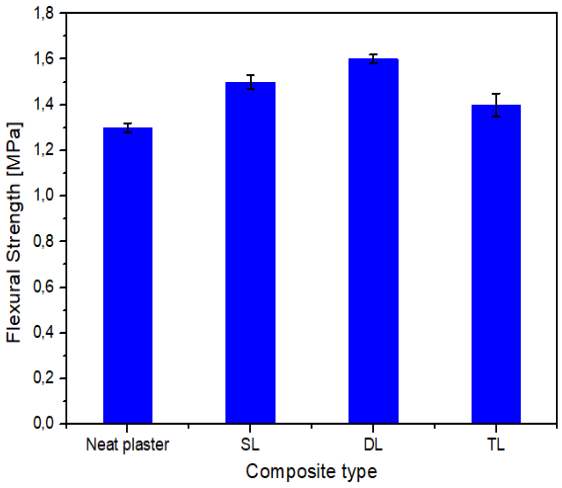

Fig. 15. Flexural strength of luffa fibers plaster composite

DOI 10.2478/ama-2023-0061

5. PHYSICAL PROPERTIES

5.1. Porosity

Fig. 16 traces the evolution of porosity of a plaster mortar reinforced with sponge luffa fibres. Note that porosity increases as a function of the percentage of spongy fibres.This refers basically to the significant vacuum resulting fromthe addition of fibres as natural layers. Porosity changes from 38% in pure plaster to 54% with a TL composite. Porosity is a very critical property that positively affects the thermal conductivity of CM. Similar observations were reported by Djoudi et al. [34].

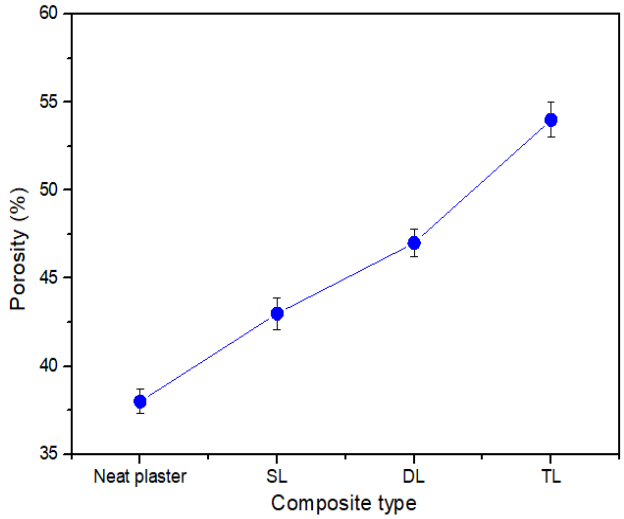

Fig. 16. Reinforcement Layers Effect on Porosity

5.2. Density

Fig.17 clarifies the variation of the density according to the layers of luffa sponge fibres. It can be therefore noted that the density decreases progressively as the layers of fibres increase. The combination density ranged from 1168 kg · m^{-3} for pure plaster to 983 kg · m^{-3} for a TL reinforcing concentration. This result goes in a good agreement with that obtained in the research of Babu et al. [33].

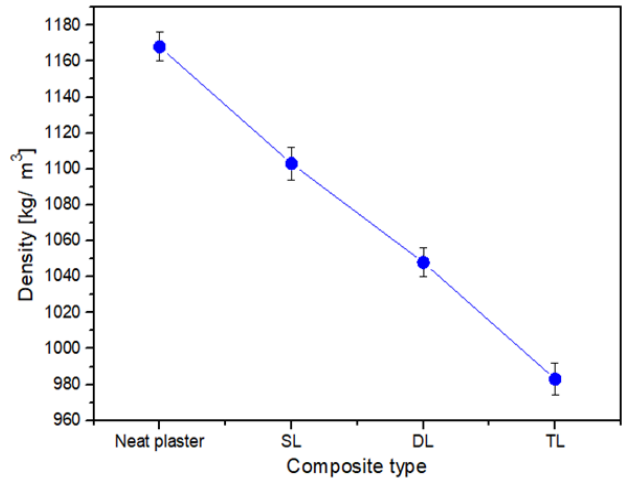

Fig. 17. Effect of reinforcement layers on density

6. THERMAL PROPERTIES

6.1. Thermal conductivity

Thermal conductivities of the various composite specimens with different layers numbers of luffa sponge fibres are displayed in Fig. 18. It is obvious that as the rate of luffa sponge fibres increases, the thermal conductivity decreases since the conductivity of CM decreases, whereas porosity increases. As far as our research is concerned, thermal conductivity of CM varies from 0.27 W · m^{-1} · K^{-1} when the material is fibreless to 0.215 W · m^{-1} · K^{-1} with a TL composite. It's worth noting that with the TL, CM displays the best thermal behaviour and the lowest density. The obtained results go in good consistency with the studies [38, 34], which confirmed that the thermal insulation of CM significantly improved with the increase of natural fibres in the base material. Similarly, Touil et al. [28] investigated the influence of alpha fibres on plaster thermal properties.

The results corroborated that by increasing the fibre concentration in both cases, the thermal properties cansignificantly improve. In terms of thermal performance, the sandwich structure proved to be noticeably more effective since an optimal thermal conductivity of 0.227 W · m^{-1} · K^{-}1 was obtained with 4% of fibres as opposed to 0.25 W · m^{-1} · K^{-1} which was achieved with the second model.

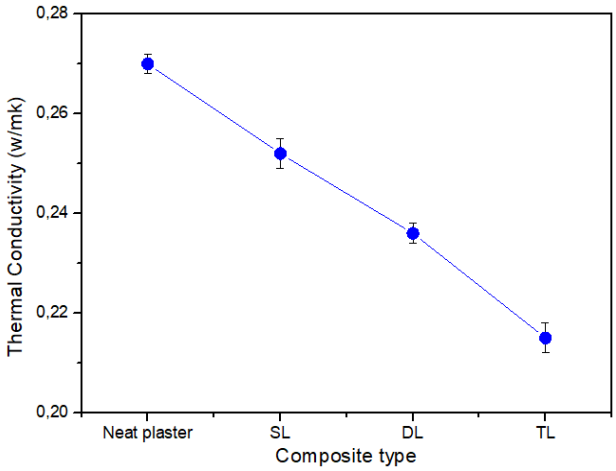

Fig. 18. The effects of luffa fibers layers of thermal conductivity

6.2. Thermal diffusivity

In Fig. 19, we inferred that the addition of fibre mats decreases the thermal diffusivity of the CM. It varies from 2.8. 10^{-7} (m^2 · s^{-1}) for the specimen without fibres to 2.49. 10^{-7} (m^2 · s^{-1}) for the specimen the TL composite. It has been proved that the increment of the fibre layer proportion reduces the thermal diffusivity. In addition, it has the merit of being a natural, safe and less-expensive product. Therefore, the more luffa sponge fibre layers exist in the medium, the less heat transfer there is. According to this significant result, the thermal insulation material not only displays a low thermal conductivity but also delays heat transfer. It is clear that the thermal diffusivity value of the composite depends on the porosity of the matrix. Likewise, Amara et al. [35] confirmed that the thermal diffusivity of date palm fibre reinforced gypsum was reduced as compared with pure gypsum.

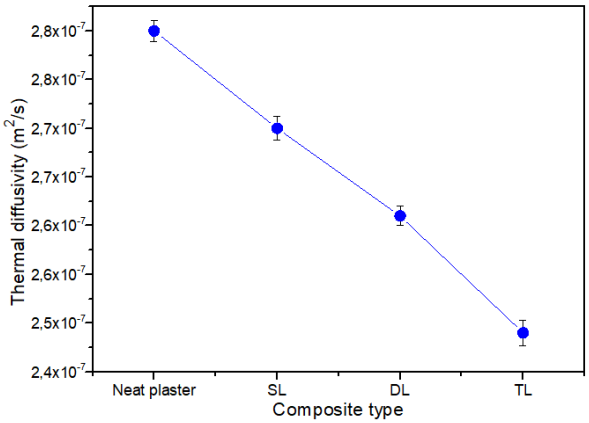

Fig. 19. Variation of the thermal diffusivity of plaster for the number of layers of luffa fibers

6.3. Thermal effusivity

Variation of thermal effusivity is plotted in Fig. 20. It indicates that the thermal effusivity of the CMs goes down accordingly with the rise of the number of luffa fibres mats in the plaster matrix. It can drop to 15.56% when the reinforcement fibres mats are at their maximum with a number of TLs. It is inferred that the plaster reinforced with luffa sponge fibres displays a certain weakness in exchanging heat with its environment as compared with the pure plaster. A similar finding was recorded by Djoudi et al. [36] and Boumhaout et al. [37] who tackled gypsum reinforced with the date palm fibre mesh.

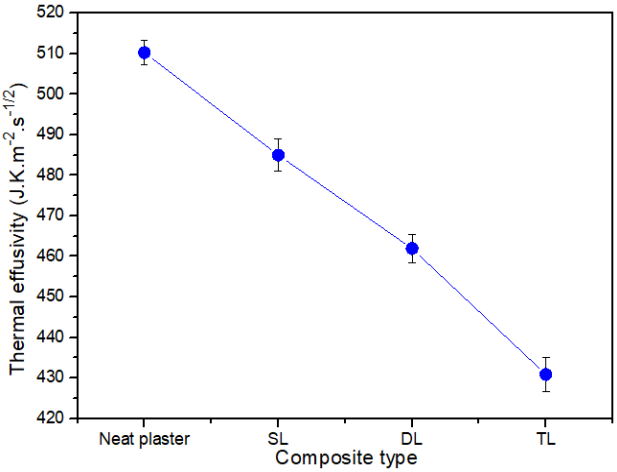

Fig. 20. Effect of reinforcement layers on thermal effusivity

6.4. The specific heat capacity

Fig. 21 traces the evolution of the specific heat capacity of the plaster reinforced with a luffa sponge fibre mats. It is noteworthy that the specific heat capacity rises to 6.4%. This increase refers to the combined effects of thermal conductivity, density and thermal diffusivity. The specific heat capacity rises from 825.58 ($J \cdot kg^{-}1 \cdot K^{-}1$) in pure plaster to 878.39 ($J \cdot kg^{-}1 \cdot K^{-}1$) with TL reinforcement mats.

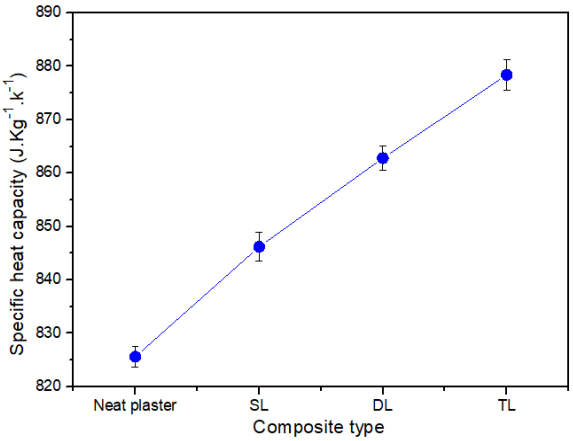

Fig. 21. Reinforcement Layers Effect on thermal capacity

7. CONCLUSION

This work contributes to the public issue of sustainable development, which has triggered significant scientific concern and whetted the widest interest among researchers, as well as industrialists. From this perspective, we attempted to enhance and control the characteristics of CMs. A study was conducted on the influence of fibre layers on the thermomechanical and physical properties of this type of material.A new set of composites was successfully manufactured using luffa sponge fibre reinforced plaster composites.

In terms of mechanical properties, the flexural strength is equal to a maximum value of 1.6 MPa at the DL. The analysis of results revealed that the thermal conductivity decreasedwhen the layer of luffa sponge fibres increased. The most insulating specimen observed far TL luffa sponge fibres to the composite yielded optimal results: with a conductivity equal to 0.215 ($Wm^{-1} \cdot K^{-1}$) and a diffusivity equal to 2.49 $10^{-7} \cdot (m^2 \cdot s^{-1})$. At this stage of analysis, we would assert that this CM based on plasters reinforced with luffa sponge fibre layers has significant thermal properties that contribute to lower energy consumption in the building process.

REFERENCES

1. Gartner Ellis M. Cohesion and expansion in polycrystalline solids formed by hydration reactions the case of gypsum plasters. Cem. Concr. 2009; 39 (4): 289-295.
2. Khalil AA, Tawfik A, Hegazy AA. Plaster composites modified morphology with enhanced compressive strength and water resistance characteristics. Constr. Build. Mater. 2018; 167: 55-64.
3. Kondratieva N, Barre M, Goutenoire F, Sanytsky M. Study of modified gypsum binder. Constr. Build. Mater. 2017; 149: 535-542.
4. Shim H, Choi GJ. Study of construction convergence technology for performance improvement in functional building materials. Build. Eng. 2017; 11:108–114.
5. Tesfaye T, Sithole B, Ramjugernath D, Mokhothu T. Valorisation of chicken feathers: Characterisation of thermal, mechanical and electrical properties, Sustain. Chem. Pharm. 2018; 9: 27–34.
6. Acda MN. Waste chicken feather as reinforcement in cement-bonded composites. Philippine J. Sci. 2010; 139 (2): 161-166.
7. Wahab ESA., Osmi SFC. Properties of Concrete Added with Chicken Rachis as Reinforcement, in: Appl. Mech. Mater. Trans. Tech. Publ. 2012; 147: 37–41.
8. Rames M, Palanikumar K, Reddy KH. Mechanical property evaluation of sisal–jute–glass fiber reinforced polyester composites, Compos. B. 2013; 48: 1–9.

DOI 10.2478/ama-2023-0061

9. Djoudi T, Hecini M., Scida D., Djebloun Y, Djemai HJ. Physico-mechanical characterization of composite materials based on date palm tree fibers, Nat. Fibers. 2021; 18 (6): 789-802.
10. Djoudi A, Khenfer MM, Bali A, Bouziani T. Effect of the addition of date palm fibers on thermal properties of plaster concrete, experimental study and modeling, Adhes. Sci. Technol. 2014; 28 (20): 2100-2111.
11. Saadaoui N, Rouilly A, Fares K, Rigal L. Characterization of date palm lignocellulosic by-products and self-bonded composite materials obtained thereof. Mater. Design. 2013; 50: 302–308.
12. Elbadry E. A. Agro-residues: Surface treatment and characterization of date palm tree fiber as composite reinforcement. Journal of Composites ID. 2014;2014.
13. Djoudi T, Hecini M, Scida D, Djebloun Y, Djemai H. Physico-mechanical characterization of composite materials based on date palm tree fibers. Journal of Natural Fibers, 2021; 18 (6): 789-802.
14. Bezazi A, Amroune S, Scarpa F. Analyse statistique et effet des traitements chimique sur le comportement physico-mécanique des fibres des bras de grappe des palmiers dattier. Synthèse: Revue des Sciences et de la Technologie. 2015; 31: 08–20.
15. Alcaraz JS, Belda IM, Sanchis EJ, Borrell JMG. Mechanical properties of plaster reinforced with yute fabrics. Compos. B. Eng. 2019; 178: 107390.
16. Eve S, Gomina M, Gmouh A, Samdi A, Moussa R, Orange GJ. Microstructural and mechanical behaviour of polyamide fibre-reinforced plaster composites. Eur. Ceram. Soc. 2002; 22 (13): 2269-2275.
17. Gencel O, del Coz Diaz JJ, Sutcu M, Koksal F, Rabanal FPA, Martinez-Barrera G. A novel lightweight gypsum composite with diatomite and polypropylene fibers. Constr. Build. Mater. 2016; 113: 732-740.
18. Iucolano F, Liguori B, Aprea P, Caputo D. Caputo, Evaluation of bio-degummed hemp fibers as reinforcement in gypsum plaster. Composites Part B: Engineering. 2018; 138: 149-156.
19. Basaran H, Demir A, Bagci M. The behavior of masonry walls with reinforced plaster mortar. Advances in Materials Science and Engineering. 2013; 2013.
20. Basaran H. Demir A, Bagci M, Ergun S. Experimental and numerical investigation of walls strengthened with fiber plaster. Structural engineering and mechanics: An international journal. 2015; 56 (2): 189-200.
21. Khalil A.A, Tawfik A, Hegazy AA, El-Shahat MF. Effect of some waste additives on the physical and mechanical properties of gypsum plaster composites. Constr. Build. Mater. 2014; 68: 580-586.
22. Ouakarrouch M, El Azhary K, Laaroussi N. Garoum M, Kifani-Sahban F. Thermal performances and environmental analysis of a new composite building material based on gypsum plaster and chicken feathers waste. Thermal Science and Engineering Progress. 2020; 19:100642.
23. Sakthieswaran N, Sophia M. Prosopis juliflorafibre reinforced green building plaster materials—An eco-friendly weed control technique by effective utilization. Environmental Technology & Innovation. 2020; 20: 101158.
24. Maaloufa Y, Mounir S, Khabbazi A, Kettar J. Thermal And Mechan The Plaster Reinforc Or Granula. International Journal of Civil Engineering. 2017; 8 (7).
25. Miraoui I, Jaballi S, Hassis H. Analysis of the mechanical properties of mortar reinforced with long unidirectional alfa fibers in different curing conditions, Mech. Compos. Mater. 2016; 52 (4): 545–554.
26. Salim K, Houssam A, Belaid A, Brahim H. Reinforcement of building plaster by waste plastic and glass. Procedia Structural Integrity. 2019; 17: 170-176.
27. Selamat ME, Hashim R, Sulaiman O, Kassim MHM, Saharudin NI, Taiwo OFA. Comparative study of oil palm trunk and rice husk as fillers in gypsum composite for building material. Constr. Build. Mater. 2019; 197: 526-532.
28. Touil M, Lachheb A, Saadani R, Kabiri MR, Rahmoune M. A new experimental strategy assessing the optimal thermo-mechanical properties of plaster composites containing Alfa fibers. Energy and Buildings. 2022; 262: 111984.
29. Chen Y, Su N, Zhang K, Zhu S, Zhu Z, Qin W, Yang Y, Shi Y, Fan S, Wang Z, Guo Y. Effect of fiber surface treatment on structure, moisture absorption and mechanical properties of luffa sponge fiber bundles. Industrial Crops and Products. 2018; 123: 341-352.
30. Taimur-Al-Mobaraka, Minaa MF, Gafurb MA, Ahmedb AN, Dhar SA. Im-provement in structural and mechanical properties of spongegourd natural fibers through dif-ferent common chemical treatments. International Conference on Engineering Materials and Metallurgical Engineering. 2016; 22- 24.
31. Kharrati K, Salhi M, Sliman J, Abdeljabar R. An Investigation of Thermomechanical Behavior of Tunisian Luffa Sponges' Fibers. Materials Sciences and Applications. 2022; 13 (12): 519-531.
32. Ayvazyan V. Etude de champs de température séparables avec une double décomposition en valeurs singulières: quelques applications à la caractérisation des propriétés thermophysiques des matérieux et au contrôle non destructif (Doctoral dissertation, Bordeaux. 2012; 1.
33. Babu KS, Ratnam C. Ratnam, Mechanical and thermophysical behavior of hemp fiber reinforced gypsum composites. Materials Today: Proceedings. 2021; 44: 2245-2249.
34. Djoudi A, Khenfer MM, Bali A. Performance of date palm fibres reinforced plaster concrete, International journal of physical sciences. 2012; 7(21): 2845-2853.
35. Amara I, Mazioud A, Boulaoued I, Mhimid A. Experimental study on thermal properties of bio-composite (gypsum plaster reinforced with palm tree fibers) for building insulation. International journal of heat and technology. 2017; 35 (1): 576-584.
36. Djoudi A, Khenfer MM, Bali A, Bouziani T. Effect of the addition of date palm fibers on thermal properties of plaster concrete: experimental study and modeling, J. Adhes. Sci. Technol. 2014; 28 (20): 2100–2111.
37. Boumhaout M, Boukhattem L, Hamdi H, Benhamou B, Nouh FA. Thermomechanical characterization of a bio-composite building material: Mortar reinforced with date palm fibers mesh. Construction and Building Materials. 2017; 135: 241-250.
38. Kharrati K, Salhi M, Sliman J, Abdeljabar R. Thermomechanical and Physical Properties of plaster concrete reinforced with natural fibers. Mechanics Of Advanced Composite Structures. 2023; 10 (2):295-308.
39. El Rhaffari Y, Boukalouch M, Khabbazi A, Samaouali A, Geraud Y. 2010 Conductivité et diffusivité thermiques des matériaux poreux: application aux pierres du monument historique Chellah. In Materiaux. 2010; 18.
40. Chen Y, Su N, Zhang K, Zhu S, Zhu Z, Qin W, Yang Y, Shi S, Fan Z,Wang Z, Guo Y. Effect of fiber surface treatment on structure, moisture absorption and me-chanical properties of luffa sponge fiber bundles. Industrial Crops and Products. 2018; 123: 341-352.
41. Taimur-Al-Mobaraka MF, Minaa MA, Gafurb A.N, Ahmedb, Dhar SA. Improvement in structural and mechanical properties of spongegourd natural fibers through different common chemical treatments. International Conference on Engineering Materials and Metallurgical Engineering, 2016; 22- 24.

Khaled Kharrati : https://orcid.org/0000-0001-9188-892X

Madiha Salhi: https://orcid.org/0000-0001-5263-2171

Abdelmoumen Hidouri: https://orcid.org/0009-0009-2945-6646

Ridha Abdeljabar: https://orcid.org/0009-0008-2601-3869